ACS OMEGA

Open Access

http://pubs.acs.org/journal/acsodf

Article

Thermodynamic Analysis of Eplerenone in 13 Pure Solvents at Temperatures from 283.15 to 323.15 K

Jianfang Liu,* Ting Liu, Rongrong Zhang, Sicheng Yang, Yaoyun Zhang, Chenglingzi Yi, Shuai Peng, and Qing Yang

Cite This: *ACS Omega* 2024, 9, 21333−21345

Read Online

ACCESS | Metrics & More | Article Recommendations

ABSTRACT: The solubility of eplerenone (EP) in 13 pure solvents (acetonitrile, *N*,*N*-dimethylformamide (DMF), acetone, 2-butanone, 4-methyl-2-pentanone, ethyl formate, methyl acetate, ethyl acetate, propyl acetate, butyl acetate, methyl propionate, ethyl propionate, ethanol, and 1-propanol) was determined by the gravimetric method at atmospheric pressure and various temperatures (from 283.15 to 323.15 K). The results showed that the solubility of EP in the selected solvents was positively correlated with the thermodynamic temperature, and the order of solubility of EP at 298.15 K was acetonitrile > DMF > 2-butanone > methyl acetate > 4-methyl-2-pentanone > methyl propionate > ethyl acetate > propyl acetate > ethyl formate > acetone > butyl acetate > ethanol >1-propanol. The modified Apelblat model, van't Hoff model, λh model, and polynomial empirical model were used for fitting the solubility data, and then the λh model was found to have the highest fitting accuracy with a minimum ARD of 7.0×10^{-3} and a minimum RMSD of 6.1×10^{-6}. The solvent effect between the solute and the solvent was analyzed using linear solvation energy relationship (LSER), and the enthalpy of solvation ($\Delta_{sol}H°$), entropy of solvation ($\Delta_{sol}S°$), and Gibbs free energy of solvation ($\Delta_{sol}G°$) of the dissolution process of EP were calculated by the van't Hoff model, which indicated that the dissolution process of EP in the selected solvents was endothermic, nonspontaneous, and entropy-increasing. In this work, the solubility, dissolution characteristics, and thermodynamic parameters of EP were studied, which will provide data support for the production, crystallization, and purification of EP and will provide important guidance for the crystallization optimization of EP in industry.

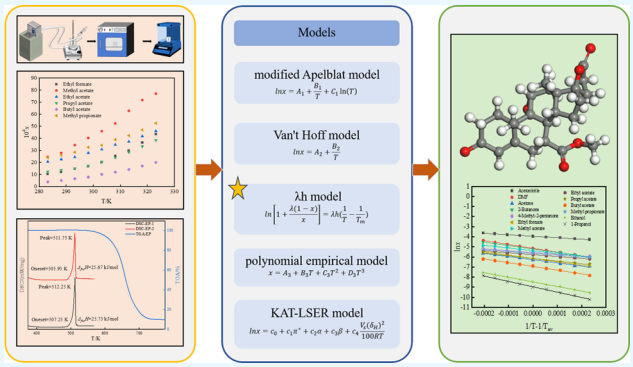

1. INTRODUCTION

Eplerenone (EP) is a novel selective aldosterone receptor antagonist first developed by Pfizer, which was initially marketed in the US in 2002 for the treatment of hypertension and heart failure.[1−3] EP, CAS No. 107724-20-9, the systematic name of 9α,11-epoxy-7α-methoxycarbonyl-3-oxo-17α-pregn-4-ene-21,17-carbolactonean, molecular formula: $C_{24}H_{30}O_6$, molecular weight: 414.49 g·mol^{-1}, is an odorless, white or off-white crystal powder, and its chemical structure and three-dimensional (3D) structure are depicted in Figure 1.[4,5]

As a novel selective aldosterone receptor antagonist, EP has stronger antagonistic effects on aldosterone than spironolactone. Additionally, it exhibits minimal affinity for androgen and progesterone receptors, leading to reduce adverse reactions. Due to its improved tolerance and fewer adverse reactions, EP can be considered an excellent alternative to spironolactone for the treatment of hypertension, heart failure, and myocardial infarction.[6,7] Pardo-Martínez et al.[8] evaluated the efficacy of spironolactone and EP in patients with heart failure and reduced ejection fraction (HFrEF) in a clinical trial in 2022,

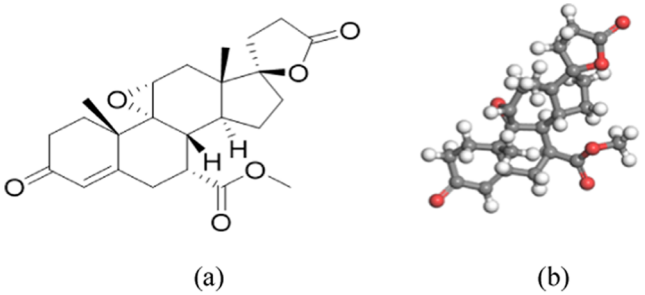

Figure 1. Chemical structure and 3D structure of EP.[4] (a) Chemical structure; (b) 3D structure.

Received: February 18, 2024
Revised: April 18, 2024
Accepted: April 23, 2024
Published: May 2, 2024

Table 1. Descriptions of the Materials Used in the Experiments

materials	CAS NO.	molecular formula	molar mass ($g \cdot mol^{-1}$)	molar volume ($cm^3 \cdot mol^{-1}$)[a]	mass fraction[b]	analysis method[c]	source
eplerenone	107724-20-9	$C_{24}H_{30}O_6$	414.49	318.84	≥0.980	HPLC	Hubei Widely Reagent Co., Ltd.
benzoic acid[d]	65-85-0	$C_7H_6O_2$	122.12	92.52	≥0.980	HPLC	Tianjin Institute of Metrology Supervision and Testing Science
sodium chloride	7647-14-5	NaCl	58.44		≥0.995	HPLC	Sinopharm Chemical Reagent Co., Ltd.
ethanol	64-17-5	C_2H_6O	46.07	58.52	≥0.997	GC	Sinopharm Chemical Reagent Co., Ltd.
1-propanol	71-23-8	C_3H_8O	60.1	74.94	≥0.995	GC	Tianjin Damao Chemical Reagent Factory
ethyl formate	109-94-4	$C_3H_6O_2$	74.08	80.83	≥0.990	GC	Tianjin Damao Chemical Reagent Factory
methyl acetate	79-20-9	$C_3H_6O_2$	74.08	79.89	≥0.980	GC	Tianjin Damao Chemical Reagent Factory
ethyl acetate	141-78-6	$C_4H_8O_2$	88.11	96.94	≥0.995	GC	Tianjin Fuyu Fine Chemical Co., Ltd.
propyl acetate	109-60-4	$C_5H_{10}O_2$	102.13	115.48	≥0.990	GC	Shanghai Macklin Biochemical Co., Ltd.
butyl acetate	123-86-4	$C_6H_{12}O_2$	116.16	132.55	≥0.990	GC	Tianjin Damao Chemical Reagent Factory
methyl propionate	554-12-1	$C_4H_8O_2$	88.11	98.59	≥0.990	GC	Shanghai Macklin Biochemical Co., Ltd.
N,*N*-dimethylformamide (DMF)	68-12-2	C_3H_7NO	73.09	77.37	≥0.995	GC	Tianjin Fuyu Fine Chemical Co., Ltd.
acetonitrile	75-05-8	C_2H_3N	41.05	52.68	≥0.995	GC	Tianjin Kermel Chemical Reagent Co., Ltd.
acetone	67-64-1	C_3H_6O	58.08	73.93	≥0.990	GC	Tianjin Damao Chemical Reagent Factory
2-butanone	78-93-3	C_4H_8O	72.11	90.20	≥0.990	GC	Tianjin Damao Chemical Reagent Factory
4-methyl-2-pentanone	108-10-1	$C_6H_{12}O$	100.16	125.76	≥0.990	GC	Sinopharm Chemical Reagent Co., Ltd.

[a]Molar volumes of 13 pure solvents were taken from the literature ,[17] and molar volumes of EP and benzoic acid were calculated by the formula (Molar volume = Molar mass/Density), whose densities were equal to 1.30 and 1.32 $g \cdot cm^{-3}$ respectively.[18,19] [b]Mass fractions of all materials were provided by the supplier. [c]Analysis methods of all materials were provided by the supplier, and no additional purification steps were performed. [d]Benzoic acid purchased was the melting point standard material GBW13233e.

and the results of the study showed that EP reduced cardiovascular mortality and all-cause mortality in patients with HFrEF compared to spironolactone. In addition, EP can be combined with other drugs. El Mokadem's team[9] found that angiotensin-converting enzyme inhibitors (ramipril) combined with mineralocorticoid receptor antagonists (EP) were effective in patients with chronic kidney disease. And the combination of ramipril and EP improved antialbuminuric effects when compared to monotherapy. In recent years, researchers have found that EP may be used to treat chronic central serous chorioretinopathy,[10] but the role of EP in this regard was controversial. Katrin Fasler's research group[11] reported that there was no evidence of efficacy of EP on subretinal fluid (SRF) regression in patients with acute and chronic central serous chorioretinopathy (CSCR) in clinical trials, and this study was still under exploration. Nowadays, studies on EP have mainly focused on clinical observation and treatment, chemical synthesis, and the pharmacological and biological activities of drugs.[6,12] However, the solubility and thermodynamic properties of EP in organic solvents have not been reported. Solubility is the physicochemical property of drugs which is crucial for the bioavailability of drugs in the human body. Moreover, studying the solubility of drugs in different solvents can provide effective data support and reference for subsequent industrial production and crystallization process research. Therefore, it is necessary to study the solid−liquid equilibrium of EP. Currently, the methods for the determination of solubility primarily include gravimetry, spectroscopy, chromatography, and dynamic laser monitoring. Bhola et al.[13] used gravimetric methods to determine the solubility of benzethonium chloride (BTC) in 9 pure solvents and two mixed solvents. Daniela's group[14] adopted UV−vis spectrophotometry to determine the solubility of isoniazid in nine (PEG 200 + water) cosolvent mixtures and calculated thermodynamic solution, mixing, and transfer functions, which showed that solution entropy was beneficial to the solution dissolution process. Cheng[15] exploited high-performance liquid chromatography (HPLC) to determine the solubility of esculetin in 10 single solvents and concluded that it was highest in methanol and lowest in water. Vahid[16] measured the solubility of ketoconazole in a mixed solvent of propylene glycol and ethanol by a laser monitoring technique in the temperature range of 293.2 to 313.2 K.

In this paper, the solubility of EP was investigated. Under atmospheric pressure and temperatures ranging from 283.15 to 323.15 K, the solubility of EP in 13 pure solvents (acetonitrile, *N*,*N*-dimethylformamide (DMF), acetone, 2-butanone, 4-methyl-2-pentanone, ethyl formate, methyl acetate, ethyl acetate, propyl acetate, butyl acetate, methyl propionate, ethanol, and 1-propanol) was determined by the gravimetric method. Four thermodynamic models (such as the modified Apelblat model, van't Hoff model, λh model, and polynomial empirical model) were employed to fit the solubility data. The model that exhibited a better fitting degree was selected. Furthermore, the solvent effect between solutes was analyzed by linear solvation energy relationship, and according to the van't Hoff model, the thermodynamic properties of the dissolution process of EP were obtained.

2. EXPERIMENTAL SECTION

2.1. Material. The raw material for the experiment, eplerenone (purity ≥98%), was purchased from Hubei Widely Reagent Co., Ltd. in China, and other analytical research-grade organic reagents are listed in Table 1 for details. The selected

https://doi.org/10.1021/acsomega.4c01550
ACS Omega 2024, 9, 21333−21345

solvents were commonly used organic solvents, and the chosen temperature fell within the optimal range for industrial production. Studying the solubility of EP in various solvents under conditions of 283.15 to 323.15 K could provide valuable insights for practical production and crystallization. Some analysis methods used for materials, such as high-performance liquid chromatography (HPLC) and gas chromatography (GC), were provided by the supplier.

2.2. Characterization Methods. *2.2.1. Differential Scanning Calorimetry (DSC) and Thermal Gravimetric Analysis (TGA).* The melting temperature (T_m) of EP was determined by using a differential scanning calorimeter (DSC 204 HP, NETZSCH, Germany) under the following conditions: EP sample weight: 5−10 mg, nitrogen flow rate: 20 mL/min, heating rate: 10 K/min, and temperature range: 298.15 to 573.15 K.

A thermal gravimetric analyzer (METTLER TOLEDO) was used to determine whether the weightless decomposition of EP occurred prior to the melting peak, and the determination conditions were the same as DSC, but the temperature range was 303.15 to 873.15 K.

2.2.2. Powder X-ray Diffraction (PXRD). PXRD could make sure whether the crystal structure of EP changes when dissolved in various solvents. The test samples were the solid−liquid mixtures that remained in the system after reaching solid−liquid phase equilibrium, which were dried in a vacuum drying oven at −0.09 MPa and 60 °C and were milled before testing. The X-ray diffractometer (model: SmartLab SE) of Rigaku Company in Japan was used in this experiment. The measurement conditions included a Cu target, tube voltage of 40 kV, tube current of 40 mA, test angle range of 5−80°, and scanning step length of 0.02°.

2.3. Solubility Determination. The solubility of EP in 13 pure solvents (acetonitrile, DMF, acetone, 2-butanone, 4-methyl-2-pentanone, ethyl formate, methyl acetate, ethyl acetate, propyl acetate, butyl acetate, methyl propionate, ethanol, and 1-propanol) was determined by the gravimetric method[13,20] over the temperature range from 283.15 to 323.15 K under atmospheric pressure. All test temperatures were controlled by a cryogenic bath (DHC-1005-A, Hangzhou Qiwei Co., Ltd.) with an error of ±0.05 K. The cryogenic bath was turned on and the test temperature was set; 30 mL of the solvent and excessive EP were added into the glass jacket crystallizer after the temperature was constant. Pre-experiments indicate that the solution reaches a saturated state after stirring for 10 h at a constant temperature. Therefore, the solution was stirred for 10 h with a magnetic stirrer and then let to stand for 2 h at the experimental temperature. The supernatant liquid was taken with a disposable syringe and filtered through a 0.22 μm nylon filter into a beaker of known mass. To ensure accuracy and prevent data inaccuracies caused by solvent evaporation, the nylon filter and the beaker were preheated to the testing temperature before filtration. After that, the beaker with supernatant liquid was put into a vacuum drying oven to dry at 60 °C for 24 h and then weighed using an analytical balance with an accuracy of ±0.0001 g (model: FA214A, Shanghai Haosheng Scientific Instrument Co., Ltd.) until the quality of the product was unchanged. The above procedures were repeated three times, changing the temperatures or solvents to measure the next set of data. To check the stability of the device, the solubility of sodium chloride (NaCl) in water was measured first, and the experimental results are shown in Figure 2. The solubilities of NaCl in water measured by this device were consistent with the reported results.[21]

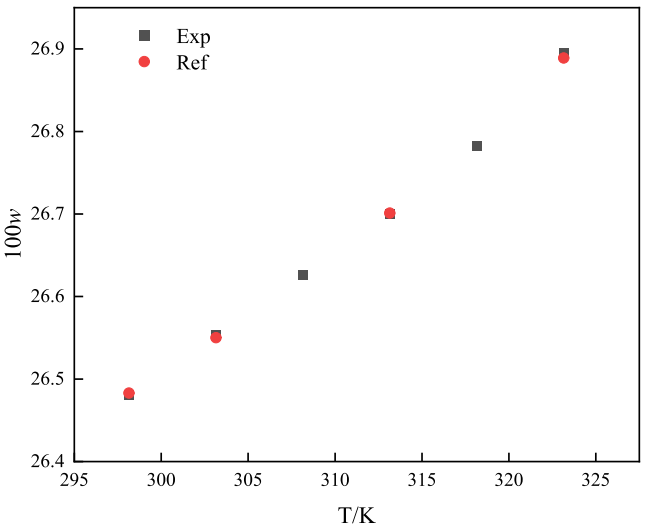

Figure 2. Experimental and literature values for the solubility of sodium chloride in water. w represents the mass fraction.

The measured solubility data were used to calculate the molar solubility (x_1) of EP in different pure solvents, according to eq 1

$$x_1 = \frac{m_1/M_1}{m_1/M_1 + m_2/M_2} \quad (1)$$

where m_1 and m_2 are the mass (g) of EP and the selected solvents, respectively; M_1 and M_2 are the molar mass (g·mol^{-1}) of EP and the selected solvents, respectively.

3. CALCULATION MODELS

3.1. Thermodynamic Models. *3.1.1. Modified Apelblat Model.* The modified Apelblat model, derived from the Clausius−Clapeyron equation, is a semiempirical thermodynamic model commonly used to describe the relationships between the molar solubility of the solute and its temperature.[22,23] The equation can be described as follows

$$\ln x_1 = A_1 + \frac{B_1}{T} + C_1 \ln(T) \quad (2)$$

The solubility data is modeled using the following equation

$$x_1 = \exp\left[A_1 + \frac{B_1}{T} + C_1 \ln(T)\right] \quad (3)$$

where x_1 is the molar solubility of EP at temperature T/K and A_1, B_1, and C_1 are model parameters. The values of A_1 and B_1 show the change in the activity coefficient, describing the effect of the nonideality of the solution on the solubility of the solute, and C_1 shows the effect of temperature on the heat of melting as a heat capacity deviation.

3.1.2. van't Hoff Model. The van't Hoff model was first proposed by Jacobus Henricus van't Hoff, which can be expressed as a two-parameter empirical model, reflecting the existence of a link between solubility and thermodynamic temperature.[13,24] And the van't Hoff model exhibits that the logarithm of the molar solubility of the solute is linearly related

https://doi.org/10.1021/acsomega.4c01550
ACS Omega 2024, 9, 21333−21345

to the reciprocal of the thermodynamic temperature. It is shown by eq 4

$$\ln x_1 = A_2 + \frac{B_2}{T} \tag{4}$$

Solve eq 4 to get the following modeling equation

$$x_1 = \exp\left(A_2 + \frac{B_2}{T}\right) \tag{5}$$

where x_1 is the molar solubility of EP at temperature T/K and A_2 and B_2 are model parameters. The values of A_2 and B_2 are model parameters related to the entropy and enthalpy of the solution.

3.1.3. λh Model. In 1980, Buchowski et al.[25] derived and proposed the λh model based on the generalized solubility equation. The λh model is a two-parameter empirical model, which is simple and suitable for associating solubility data with thermodynamic temperature.[20] The expression is as follows:

$$\ln\left[1 + \frac{\lambda(1 - x_1)}{x_1}\right] = \lambda h\left(\frac{1}{T} - \frac{1}{T_m}\right) \tag{6}$$

The modeling equation is as follows:

$$x_1 = \frac{\lambda}{\exp\left[\lambda h\left(\frac{1}{T} - \frac{1}{T_m}\right)\right] - (1 - \lambda)} \tag{7}$$

where x_1 is the molar solubility of EP at temperature T/K, T_m is the melting point of EP, λ, and h are model parameters, the value of λ represents the nonideality of the solution system, and h represents the enthalpy of the solution.

3.1.4. Polynomial Empirical Model. The polynomial empirical model can be applied to correlate and fit the solubility data. Additionally, the molar solubility of solute is a function of temperature when the external influence conditions are fixed,[26,27] which is expressed as

$$x_1 = A_3 + B_3T + C_3T^2 + D_3T^3 \tag{8}$$

where x_1 is the molar solubility of EP at temperature T/K and A_3, B_3, C_3, and D_3 are model parameters.

3.2. Evaluation Criteria of Models. The average relative deviation (ARD) and root-mean-square deviation (RMSD) are regularly used to evaluate the accuracy of the fitting results of thermodynamic models and their corresponding formulas as follows:

$$\mathrm{ARD} = \frac{1}{N}\sum_{i=1}^{N}\left|\frac{x_1 - x_{cal}}{x_1}\right| \tag{9}$$

$$\mathrm{RMSD} = \sqrt{\frac{\sum_{i=1}^{N}(x_1 - x_{cal})^2}{N}} \tag{10}$$

where N represents the number of data points, x_1 represents the experimentally observed value, and x_{cal} represents the predicted value from the model.

3.3. KAT-LSER Model. The linear solvation energy relationship (LSER) is a quantitative structure−activity relationship (QSAR) model used to describe the solvent effect of solute−solvent interactions on the dissolution process.[28] At present, the LSER model has been successfully applied to predict the solubility of substances, octanol/water partition coefficient, and various biological toxicity properties.[29] The LSER model explains solvent effects by dividing solvent−solvent interactions into specific (such as hydrogen bond force) and nonspecific (including electrostatic force, dipole−dipole force, dipole−induced dipole force, and dispersion force) interactions.[30] The Gibbs free energy (XYZ) during dissolution is the sum of solute−solvent interaction energy and cavity creation energy,[31−33] as shown in eq 11

$$XYZ = XYZ_0 + \sum \text{Solute} - \text{Solvent Interaction Energy} + \text{Cavity Creation Energy} \tag{11}$$

where XYZ_0 is the intercept of the equation, which is only related to the properties of the solvent.

In the 1980s, Kamlet et al.[31] developed the KAT-LSER model by analyzing the solubility data in conjunction with the solvent properties, which explains the change of Gibbs free energy during the dissolution process from multiple perspectives. The KAT-LSER model is expressed as follows

$$\ln x_1 = c_0 + c_1\pi^* + c_2\alpha + c_3\beta + c_4\frac{V_s(\delta_H)^2}{100RT} \tag{12}$$

where x_1 is the molar solubility of EP at temperature T/K, π^*, α, and β are denoted as polarity/dipolarity of the solvent, summation of the hydrogen bond donor propensities of the solvent, and summation of the hydrogen bond acceptor propensities of the solvent, respectively. V_s is the molar volume of the solvent (cm^3/mol), δ_H is the Hildebrand solubility parameter, and R is the molar constant of the gas (which takes the value of 8.314 J/(mol·K). The conversion of δ_H to $V_s(\delta_H)^2/(100RT)$ is to make it dimensionless and within a certain range with the other three properties. In the equation, c_0 is the intercept of the model when $\pi^* = \alpha = \beta = \delta_H = 0$. c_1 and c_4 denote the sensitivities of the solute−solvent and the solvent−solvent via nonspecific electrostatic interactions, while c_2 and c_3 represent the interactions of the solute−solvent through the specific hydrogen-bonding interactions.

3.4. Thermodynamic Properties of the Solution. The solubility of a solute is closely related to the thermodynamic properties of solutions. To investigate the thermodynamic behavior of the dissolution process between EP and pure solvents, several thermodynamic parameters such as standard enthalpy of dissolution ($\Delta_{sol}H^\circ$), standard entropy of dissolution ($\Delta_{sol}S^\circ$), and standard Gibbs free energy of dissolution ($\Delta_{sol}G^\circ$) can be analyzed.[24,34,35] The standard enthalpy of dissolution ($\Delta_{sol}H^\circ$) can be calculated according to the van't Hoff model, as shown in eq 13

$$\ln x_1 = \frac{-\Delta_{sol}H^\circ}{R}\left(\frac{1}{T} - \frac{1}{T_{av}}\right) + b \tag{13}$$

$$T_{av} = \frac{N}{\sum_{i=1}^{N}\frac{1}{T_i}} \tag{14}$$

where x_1 is the molar solubility of EP at temperature T/K and T_{av} is the average harmonic temperature of the experiment. From eq 13, $\ln x_1$ is linearly related to $(1/T - 1/T_{av})$, and the slope of the curve is $(-\Delta_{sol}H^\circ)/R$ with an intercept of b, as obtained by graphing with the software.

The equations of standard entropy of dissolution ($\Delta_{sol}S^\circ$) and standard Gibbs free energy of dissolution ($\Delta_{sol}G^\circ$) are expressed as eqs 15 and 16, respectively.

$$\Delta_{sol}G^\circ = -R \times T_{av} \times b \tag{15}$$

https://doi.org/10.1021/acsomega.4c01550
ACS Omega 2024, 9, 21333−21345

$$\Delta_{sol}S^{\circ} = \frac{\Delta_{dis}G^{\circ} - \Delta_{dis}H^{\circ}}{T_{av}} \quad (16)$$

To compare the contribution of $\Delta_{sol}H^{\circ}$ and $\Delta_{sol}S^{\circ}$ to Gibbs free energy, the relative contribution of enthalpy (ξ_H/%) and entropy (ξ_{TS}/%)[36,37] during the dissolution process can be calculated by eqs 17 and 18.

$$\xi_H/\% = \frac{|\Delta_{sol}H^{\circ}|}{|\Delta_{sol}H^{\circ}| + |T_{av}\Delta_{sol}S^{\circ}|} \times 100 \quad (17)$$

$$\xi_{TS}/\% = \frac{|T_{av} \times \Delta_{dis}S^{\circ}|}{|\Delta_{sol}H^{\circ}| + |T_{av}\Delta_{sol}S^{\circ}|} \times 100 \quad (18)$$

4. RESULTS AND DISCUSSION

4.1. Characterizations of EP. *4.1.1. DSC and TGA.* The calibration material of DSC in this paper was benzoic acid, the standard material of melting point, which was measured three times according to the steps in Section 2.2.1. The average melting point and melting enthalpy ($\Delta_{fus}H$) of benzoic acid were 395.65 K and 16.49 kJ/mol, respectively, and the standard uncertainties of melting point and melting enthalpy of benzoic acid were 0.05 K and 0.28 kJ/mol, respectively. The melting point and melting enthalpy ($\Delta_{fus}H$) of benzoic acid in the literature[38] were 395.40 K and 17.1 kJ/mol, respectively. The relative deviation was less than 4%, indicating that the device was reliable.

The DSC and TGA curves of EP are presented in Figure 3, and it could be found that there is no weightless

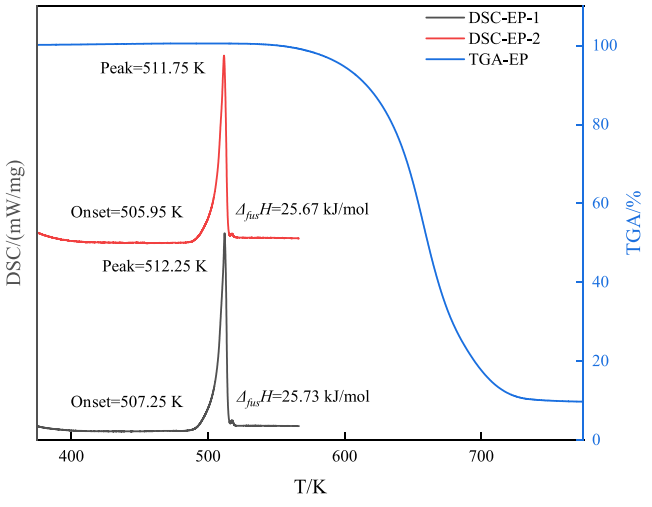

Figure 3. DSC and TGA curves of EP.

decomposition of EP before the endothermic peak. And EP had an endothermic melting peak (T_p) at 512.00 K, and its standard uncertainty was 0.25 K. In addition, EP had another endothermic melting peak at 517.85 K. The test results were similar to the literature results.[39] The average melting point (T_m) and average melting enthalpy ($\Delta_{fus}H$) of EP obtained by DSC analysis software were 506.60 K and 25.70 kJ/mol, respectively, and their standard uncertainties were 0.65 K and 0.03 kJ/mol, respectively. Due to the different experimental conditions, environment, and sample sources, there were some deviations between the test and the literature results.

4.1.2. PXRD. EP raw material and EP recovered from solvents were analyzed by PXRD, and since the characteristic peak positions of EP were mainly concentrated at 5 to 35°, only the spectra of 5 to 35° are shown in Figure 4. It was clear

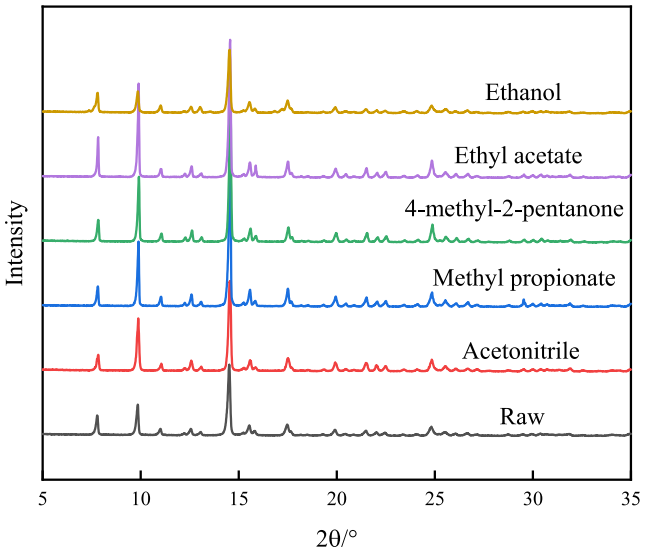

Figure 4. PXRD patterns of raw material and EP recovered from solvents.

that the characteristic peak position of EP recovered from solvents was consistent with that of the raw material, indicating that the crystalline form of EP had not been transformed in the process of dissolution. But the peak strength changed, which may be due to factors such as the roughness of the crystal surface, the presence of defects on the crystal surface, and the degree of crystallinity.

4.2. Solubility Results. The trends of solubility of EP in 13 pure solvents are plotted in Figure 5. The fitting curve in Figure 5 was obtained by fitting the polynomial empirical model. And the solubility and the fitted data are listed in Table 2. From Table 2, it could be found that the solubility of EP in 13 solvents increased with an increase in temperature. However, the influence of temperature on the solubility of each solvent was not uniform, so some same kinds of solvents had an increasing difference in solubility as the temperature increased. In addition, the solubility sequence of EP at 298.15 K was acetonitrile > DMF > 2-butanone > methyl acetate > 4-methyl-2-pentanone > methyl propionate > ethyl acetate > propyl acetate > ethyl formate > acetone > butyl acetate > ethanol > 1-propanol. Within the experimental range, EP had the maximum molar solubility in acetonitrile solution (2.67×10^{-2}, 323.15 K) and the minimum molar solubility in 1-propanol solution (3.65×10^{-5}, 283.15 K).

Moreover, Figure 5a revealed that the solubility of EP in ester (R_1COOR_2) solvents decreased with the increase of R_2. The solubility of EP in methyl acetate increased significantly more than that of several other esters with the rising temperature. The order of solubility of EP in six ester solvents was methyl acetate > methyl propionate > ethyl acetate > propyl acetate > ethyl formate > butyl acetate. According to Figure 5b, the solubility sequence of EP in the three ketone solvents was 2-butanone > 4-methyl-2-pentanone > acetone; the solubility of EP in ketone (CH_3COR_1) solvents increased with the increase of R_1 but decreased if R_1 had branched chains. At lower temperatures, the solubility of 4-methyl-2-pentanone was close to 2-butanone. But with the increase of temperature, the solubility of 4-methyl-2-pentanone was much

https://doi.org/10.1021/acsomega.4c01550
ACS Omega 2024, 9, 21333−21345

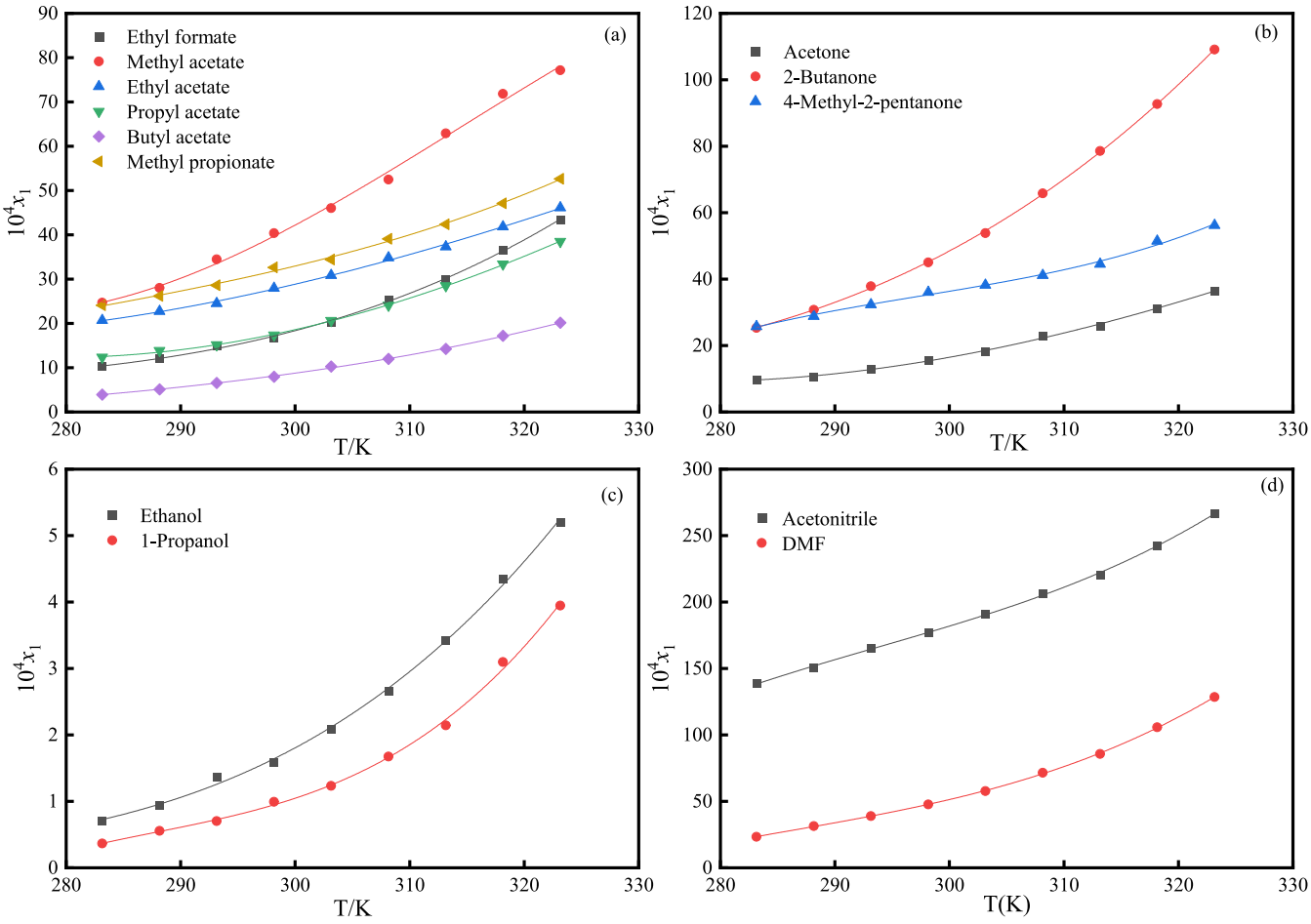

Figure 5. Molar solubility of EP in 13 pure solvents. (a) Ester solvents, (b) ketone solvents, (c) alcohol solvents, and (d) others.

lower than 2-butanone. As shown in Figure 5c, with the growth of the carbon chain, the solubility of EP in alcoholic solvents became smaller. The order of solubility of EP in both alcoholic solvents was ethanol > 1-propanol. Lastly, as shown in Figure 5d, the solubility of EP in acetonitrile was higher than DMF.

The physical properties of the 13 organic solvents such as boiling point (bp), polarity/dipolarity (π^*), dipole moment (μ), dielectric constant (ε), hydrogen bond donor capacity (α), hydrogen bond acceptor capacity (β), and Hildebrand solubility parameters (δ_H) are listed in Table 3. The order of boiling points was DMF > butyl acetate > 4-methyl-2-pentanone > propyl acetate > 1-propanol > acetonitrile > 2-butanone ≈ methyl propionate > ethanol > ethyl acetate > methyl acetate > acetone > ethyl formate; the polarizability of solvents obeyed the order as DMF > acetonitrile > acetone > 4-methyl-2-pentanone > ethyl formate > methyl acetate > ethyl acetate > ethanol > 1-propanol > propyl acetate > butyl acetate; the order of dipole moments was acetonitrile > DMF > acetone > 4-methyl-2-pentanone > 2-butanone > ethyl formate = butyl acetate > propyl acetate > ethyl acetate > methyl acetate > ethyl acetate > ethanol > 1-propanol; dielectric constant was ranked as DMF > acetonitrile > ethanol > 1-propanol > acetone > 2-butanone > 4-methyl-2-pentanone > ethyl formate > methyl acetate > ethyl acetate > propyl acetate > butyl acetate; and the cohesion energy density was ethanol > 1-propanol > acetonitrile > DMF > acetone > methyl acetate > ethyl formate > 2-butanone > methyl propionate > ethyl acetate > 4-methyl-2-pentanone > propyl acetate > butyl acetate.

However, the experimental results were inconsistent with the above four orders, indicating that there was no obvious correlation between the solubility of EP and the above orders of the physical properties of solvents. This phenomenon showed that the dissolution process of EP in different solvents was very complicated. The solubility of EP was not affected by a single factor but may be influenced by many factors. These factors may include the physical and chemical properties of solute and solvents, intermolecular forces (such as hydrogen bond, dispersion force, induction force, orientation force), molecular structure, and stereoscopic effects.

4.3. Evaluations of Models. The adjusted R^2, model parameters, ARD, and RMSD of the four models are shown in Tables 4−6. As can be seen from Tables 4−6, the adjusted R^2 of the four models was close to 1, and the maximum ARD values were 3.27×10^{-2}, 4.70×10^{-2}, 4.68×10^{-2}, and 2.37×10^{-2}, respectively. The maximum RMSD values were 1.664×10^{-4}, 2.95×10^{-4}, 2.392×10^{-4}, and 1.006×10^{-4}, respectively. The above data indicated that the four models can effectively describe the relationship between the solubility of EP and temperature. In combination with the total ARD and RMSD, the polynomial empirical model exhibited higher fitting accuracy and smaller error compared to the modified Apelblat model, van't Hoff model, and λh model. However, some parameters in the modified Apelblat model, van't Hoff model, and polynomial empirical model were not significant

https://doi.org/10.1021/acsomega.4c01550
ACS Omega 2024, 9, 21333−21345

Table 2. Experimental and Fitting Data of Molar Solubility of EP in 13 Pure Solvents at Temperatures from 283.15−323.15 K and Pressure 101.3 kPa[a,b]

T/K	$10^4 x_1^{exp}$	$10^4 x_1^{Apelblat}$	$10^4 x_1^{van'tHoff}$	$10^4 x_1^{\lambda h}$	$10^4 x_1^{polynomial}$
			Ethyl Formate		
283.15	10.3252	10.1607	9.4000	9.4328	10.3967
288.15	12.0202	12.1064	11.6335	11.6579	12.0973
293.15	14.8700	14.4605	14.2933	14.3069	14.3165
298.15	16.8370	17.3108	17.4403	17.4416	17.1436
303.15	20.2534	20.7638	21.1411	21.1302	20.6681
308.15	25.3326	24.9491	25.4675	25.4475	24.9795
313.15	29.9784	30.0244	30.4976	30.4755	30.1671
318.15	36.6205	36.1812	36.3147	36.3043	36.3205
323.15	43.3808	43.6519	43.0085	43.0325	43.5289
			Methyl Acetate		
283.15	24.6822	23.8355	24.8952	25.0074	24.7655
288.15	27.9883	28.7029	29.2930	29.3547	28.4687
293.15	34.4863	34.1599	34.2769	34.2854	33.5278
298.15	40.3703	40.2059	39.8980	39.8561	39.6875
303.15	46.0086	46.8298	46.2088	46.1271	46.6924
308.15	52.4982	54.0097	53.2633	53.1635	54.2872
313.15	62.8985	61.7130	61.1170	61.0348	62.2166
318.15	71.8265	69.8973	69.8262	69.8160	70.2251
323.15	77.1693	78.5112	79.4482	79.5882	78.0576
			Ethyl Acetate		
283.15	20.6757	20.4522	20.0454	20.2062	20.6293
288.15	22.7423	22.6862	22.5037	22.5833	22.6235
293.15	24.5364	25.1507	25.1641	25.1680	25.0074
298.15	27.9556	27.8673	28.0336	27.9743	27.7542
303.15	30.8534	30.8595	31.1194	31.0171	30.8373
308.15	34.8187	34.1525	34.4279	34.3130	34.2298
313.15	37.3006	37.7738	37.9656	37.8798	37.9049
318.15	41.8303	41.7530	41.7382	41.7372	41.8359
323.15	46.1055	46.1221	45.7513	45.9066	45.9961
			Propyl Acetate		
283.15	12.3694	12.0194	10.9726	11.0363	12.5370
288.15	13.8637	13.6339	13.0587	13.1014	13.5120
293.15	15.1359	15.5719	15.4494	15.4686	15.1939
298.15	17.3686	17.8986	18.1750	18.1703	17.5551
303.15	20.6262	20.6937	21.2672	21.2416	20.5676
308.15	24.0728	24.0547	24.7589	24.7201	24.2037
313.15	28.5204	28.1010	28.6843	28.6466	28.4357
318.15	33.3844	32.9790	33.0786	33.0652	33.2356
323.15	38.4751	38.8677	37.9783	38.0236	38.5758
			Butyl Acetate		
283.15	3.9511	4.0077	4.2634	4.2754	3.9261
288.15	5.1100	5.1390	5.3071	5.3151	5.1452
293.15	6.5641	6.4912	6.5571	6.5601	6.5375
298.15	7.9483	8.0839	8.0443	8.0417	8.1316
303.15	10.2477	9.9337	9.8025	9.7946	9.9564
308.15	12.0042	12.0539	11.8686	11.8570	12.0406
313.15	14.2454	14.4533	14.2826	14.2714	14.4130
318.15	17.1843	17.1363	17.0879	17.0844	17.1024
323.15	20.1350	20.1021	20.3311	20.3472	20.1374
			Methyl Propionate		
283.15	24.0936	24.0650	23.1973	23.3920	23.9443
288.15	26.1842	26.3305	25.9522	26.0493	26.3785
293.15	28.5936	28.8820	28.9234	28.9302	28.9780
298.15	32.6294	31.7537	32.1177	32.0494	31.8227
303.15	34.3830	34.9841	35.5417	35.4229	34.9924
308.15	39.0631	38.6169	39.2018	39.0681	38.5670
313.15	42.3920	42.7011	43.1036	43.0038	42.6261
318.15	47.1056	47.2918	47.2526	47.2509	47.2498
323.15	52.6321	52.4511	51.6538	51.8323	52.5178

https://doi.org/10.1021/acsomega.4c01550
ACS Omega 2024, 9, 21333−21345

Table 2. continued

T/K	$10^4 x_1^{exp}$	$10^4 x_1^{Apelblat}$	$10^4 x_1^{van'tHoff}$	$10^4 x_1^{\lambda h}$	$10^4 x_1^{polynomial}$
			Acetone		
283.15	9.8301	9.1744	8.8552	8.8907	9.6448
288.15	10.5105	10.9881	10.7952	10.8196	10.8829
293.15	12.8691	13.1322	13.0716	13.0827	12.8059
298.15	15.5404	15.6615	15.7269	15.7236	15.3725
303.15	18.2994	18.6394	18.8064	18.7898	18.5413
308.15	22.9550	22.1385	22.3588	22.3333	22.2709
313.15	25.9253	26.2421	26.4357	26.4105	26.5202
318.15	31.2586	31.0457	31.0919	31.0829	31.2476
323.15	36.5097	36.6584	36.3851	36.4176	36.4120
			2-Butanone		
283.15	25.3266	25.1259	24.9352	24.9884	25.4650
288.15	30.7864	30.7883	30.6692	30.7060	30.7507
293.15	37.8333	37.4975	37.4564	37.4729	37.2898
298.15	45.0327	45.4046	45.4399	45.4341	45.1953
303.15	53.8321	54.6759	54.7747	54.7481	54.5800
308.15	65.8053	65.4943	65.6281	65.5871	65.5568
313.15	78.5798	78.0595	78.1795	78.1387	78.2385
318.15	92.7111	92.5894	92.6204	92.6059	92.7381
323.15	109.0753	109.3205	109.1547	109.2085	109.1684
			4-Methyl-2-pentanone		
283.15	25.7568	26.4928	25.6915	25.9085	25.5549
288.15	28.8281	28.9381	28.5993	28.7032	29.2948
293.15	32.3161	31.6656	31.7199	31.7210	32.4338
298.15	36.0587	34.7064	35.0591	34.9762	35.2925
303.15	38.2014	38.0949	38.6220	38.4843	38.1916
308.15	41.1332	41.8694	42.4137	42.2622	41.4515
313.15	44.5408	46.0724	46.4384	46.3286	45.3929
318.15	51.4835	50.7513	50.7004	50.7039	50.3364
323.15	56.2323	55.9586	55.2034	55.4106	56.6025
			Ethanol		
283.15	0.7097	0.7104	0.7423	0.7436	0.7263
288.15	0.9442	0.9534	0.9774	0.9784	0.9579
293.15	1.3627	1.2616	1.2748	1.2755	1.2581
298.15	1.5867	1.6476	1.6481	1.6482	1.6404
303.15	2.0927	2.1250	2.1127	2.1121	2.1184
308.15	2.6624	2.7084	2.6865	2.6853	2.7054
313.15	3.4184	3.4136	3.3900	3.3887	3.4150
318.15	4.3549	4.2569	4.2466	4.2459	4.2606
323.15	5.2062	5.2554	5.2826	5.2843	5.2559
			1-Propanol		
283.15	0.3654	0.3956	0.3471	0.3474	0.3683
288.15	0.5539	0.5278	0.4879	0.4882	0.5460
293.15	0.7011	0.7045	0.6780	0.6782	0.7265
298.15	0.9919	0.9405	0.9317	0.9319	0.9475
303.15	1.2321	1.2557	1.2670	1.2671	1.2469
308.15	1.6722	1.6763	1.7060	1.7058	1.6622
313.15	2.1431	2.2373	2.2752	2.2750	2.2313
318.15	3.0962	2.9847	3.0071	3.0069	2.9919
323.15	3.9465	3.9799	3.9403	3.9405	3.9817
			Acetonitrile		
283.15	138.9418	140.4332	136.4462	137.5795	138.2878
288.15	150.4217	151.0072	149.4428	149.9469	151.8765
293.15	165.3174	162.7465	163.1702	163.1263	164.5486
298.15	176.6819	175.7631	177.6341	177.1640	177.1092
303.15	190.8641	190.1814	192.8392	192.1106	190.3636
308.15	206.3069	206.1396	208.7885	208.0212	205.1169
313.15	220.5818	223.7908	225.4841	224.9564	222.1744
318.15	242.4299	243.3041	242.9266	242.9828	242.3413
323.15	266.6956	264.8664	261.1157	262.1735	266.4228
			DMF		

https://doi.org/10.1021/acsomega.4c01550
ACS Omega 2024, 9, 21333−21345

Table 2. continued

T/K	$10^4 x_1^{exp}$	$10^4 x_1^{Apelblat}$	$10^4 x_1^{van'tHoff}$	$10^4 x_1^{\lambda h}$	$10^4 x_1^{polynomial}$
283.15	23.3492	24.6754	23.9144	23.9245	23.4771
288.15	31.3367	30.7435	30.2376	30.2465	31.0421
293.15	38.8070	38.1400	37.9279	37.9349	38.9126
298.15	47.7039	47.1213	47.2138	47.2183	47.7315
303.15	57.7826	57.9868	58.3502	58.3516	58.1419
308.15	71.4673	71.0851	71.6195	71.6177	70.7868
313.15	85.6799	86.8211	87.3329	87.3286	86.3092
318.15	105.7395	105.6638	105.8320	105.8270	105.3522
323.15	128.4462	128.1547	127.4894	127.4875	128.5589

[a] x_1^{exp}, $x_1^{Apelblat}$, $x_1^{van'tHoff}$, $x_1^{\lambda h}$, and $x_1^{polynomial}$ represent the experimental value and fitted value, respectively. [b] Standard uncertainties u: $u(T)$ = 0.05 K, $u(P)$ = 0.3 kPa, and relative standard uncertainty u_r: $u_r(x)$ = 0.05.

Table 3. Values of π^*, μ, ε, α, β, and δ_H for the 13 Pure Solvents at 298.15 K

solvents	bp (°C)[a]	π^*[b]	μ[b]	ε[b]	α[b]	β[b]	δ_H[c] ($J^{1/2}/cm^{3/2}$)
acetonitrile	81	0.75	3.92	35.69	0.07	0.32	24.09
DMF	153	0.88	3.82	37.22	0.00	0.74	23.97
acetone	56.5	0.71	2.88	20.49	0.04	0.49	19.77
2-butanone	79.6	0.67	2.78	18.25	0.00	0.51	18.80
4-methyl-2-pentanone	117	0.65	2.81	12.89	0.00	0.51	17.83
ethyl formate	53	0.61	1.90	8.33	0.00	0.38	18.94
methyl acetate	57	0.60	1.72	6.86	0.00	0.45	19.44
ethyl acetate	76.5	0.55	1.78	5.99	0.00	0.45	18.35
propyl acetate	102	0.50	1.80	5.52	0.00	0.45	17.67
butyl acetate	124	0.46	1.90	4.99	0.00	0.45	17.58
methyl propionate	79	0.55					18.63
ethanol	78.3	0.54	1.69	24.85	0.37	0.48	26.42
1-propanol	97	0.52	1.55	20.52	0.37	0.48	24.56

[a] The values of bp were provided by the supplier. [b] The values of π^*, μ, ε, α, and β were obtained from the literature.[40] [c] The values of δ_H were obtained from the literature.[17]

Table 4. Parameters of the Modified Apelblat Model and the van't Hoff Model (P = 101.3 kPa)[a,b]

	modified Apelblat model				van't Hoff model		
solvents	$100R^2$	A_1	B_1	C_1	$100R^2$	A_2	B_2
acetonitrile	99.77	−106.82 ± 16.53	3396.67 ± 1131.17	16.04 ± 2.48	99.39	0.95 ± 0.14	−1484.66 ± 41.52
DMF	99.94	−65.61 ± 30.79	0*	10.86 ± 4.51	99.93	7.48 ± 0.13	−3828.24 ± 40.78
acetone	99.68	−86.57 ± 52.09	0*	13.52 ± 7.71	99.67	4.39 ± 0.23	−3232.60 ± 70.09
2-butanone	99.97	0*	−2506.98 ± 1102.63	2.83 ± 3.45	99.97	5.93 ± 0.07	−3377.46 ± 21.22
4-methyl-2-pentanone	98.97	−108.79 ± 41.50	3192.74 ± 2873.15	16.22 ± 6.25	98.81	0*	−1749.62 ± 68.62
ethyl formate	99.86	−187.05 ± 20.95	5307.10 ± 2006.01	28.59 ± 3.14	99.67	5.32 ± 0.25	−3478.56 ± 76.20
methyl acetate	99.47	126.86 ± 41.01	−8277.07 ± 2843.43	−18.36 ± 6.28	99.40	3.38 ± 0.25	−2654.48 ± 77.18
ethyl acetate	99.76	−67.66 ± 27.58	0*	10.13 ± 4.12	99.69	0.45 ± 0.12	−1887.69 ± 37.64
propyl acetate	99.77	−250.72 ± 14.54	8728.10 ± 1739.13	37.76 ± 2.22	99.22	3.22 ± 0.30	−2840.19 ± 93.01
butyl acetate	99.91	153.83 ± 21.11	−10380.31 ± 1599.96	−22.14 ± 3.26	99.81	4.86 ± 0.20	−3573.26 ± 60.79
methyl propionate	99.72	−126.51 ± 20.50	3925.53 ± 1516.63	18.88 ± 3.09	99.38	0.40 ± 0.17	−1831.21 ± 51.68
ethanol	99.80	96.15 ± 55.84	−8608.78 ± 3381.69	−13.34 ± 8.58	99.81	6.35 ± 0.26	−4489.01 ± 80.02
1-propanol	99.70	−223.79 ± 47.10	0*	34.60 ± 7.00	99.65	9.36 ± 0.45	−5557.32 ± 138.58

[a] Standard uncertainty $u(P)$ = 0.3 kPa. [b] 0* indicates that the parameter has no significance and is not statistically significant.

and did not have statistical significance, and all parameters were significant when all solubility data were only fitted with the λh model. Therefore, the λh model was selected as the predictive model for the solubility of EP in this study.

4.4. KAT-LSER Model. In this research, the KAT-LSER model was used to investigate the solvent effect of the dissolution process of EP in pure solvents and then to analyze the impact of the solvent effect on the solubility of EP. The values of π^*, α, β, and δ_H for the pure solvents are presented in Table 3.

The solubility data of EP in pure solvents measured at 298.15 K was fitted to each property of the solvents using the KAT-LSER model. The model was obtained as

$$\ln x_1 = -7.892(1.055) + 7.301(1.704)\pi^* - 6.554(1.271)\alpha - 5.283(1.970)\beta$$

$$n = 12,\ R^2 = 0.848,\ F = 21.472,\ \mathrm{RSS} = 2.577 \qquad (19)$$

where n is the number of solvent species, R^2 is adjusted R^2, F is the F-test, and RSS is the residual sum of squares.

https://doi.org/10.1021/acsomega.4c01550
ACS Omega 2024, 9, 21333−21345

Table 5. Parameters of the λh Model and the Polynomial Empirical Model (P = 101.3 kPa)[a,b]

	λh model			polynomial empirical model				
solvents	$100R^2$	λ	h	$100R^2$	A_3	B_3	C_3	D_3
acetonitrile	99.60	0.08 ± 5.88 × 10^{-3}	15759.56 ± 601.45	99.92	−2.78 ± 0.73	0.03 ± 7.20 × 10^{-3}	−9.46 × 10^{-5} ± 2.38 × 10^{-5}	1.07 × 10^{-7} ± 2.61 × 10^{-8}
DMF	99.93	0.93 ± 0.05	4130.14 ± 182.22	99.98	−2.04 ± 0.30	0.02 ± 2.94 × 10^{-3}	−7.35 × 10^{-5} ± 9.70 × 10^{-6}	8.57 × 10^{-8} ± 1.07 × 10^{-8}
acetone	99.68	0.13 ± 0.01	25325.73 ± 1859.73	99.75	0*	0*	0*	0*
2-butanone	99.97	0.46 ± 0.01	7268.96 ± 162.94	99.97	0*	2.42 × 10^{-3} ± 2.72 × 10^{-3}	−1.05 × 10^{-5} ± 8.99 × 10^{-6}	1.51 × 10^{-8} ± 9.89 × 10^{-9}
4-methyl-2-pentanone	98.97	0.02 ± 3.07 × 10^{-3}	61218.96 ± 4271.03	99.39	−1.14 ± 0.47	0.01 ± 4.63 × 10^{-3}	−3.82 × 10^{-5} ± 1.53 × 10^{-5}	4.27 × 10^{-8} ± 1.68 × 10^{-8}
ethyl formate	99.69	0.20 ± 0.02	17198.95 ± 1367.28	99.87	0*	2.41 × 10^{-3} ± 2.41 × 10^{-3}	−9.27 × 10^{-6} ± 7.97 × 10^{-6}	1.19 × 10^{-8} ± 8.77 × 10^{-9}
methyl acetate	99.35	0.14 ± 0.02	19040.70 ± 1617.46	99.49	1.02 ± 0.79	−9.95 × 10^{-3} ± 7.88 × 10^{-3}	3.21 × 10^{-5} ± 2.60 × 10^{-5}	−3.40 × 10^{-8} ± 2.8610^{-8}
ethyl acetate	99.76	0.03 ± 1.57 × 10^{-3}	65461.72 ± 2368.57	99.74	0*	0*	0*	0*
propyl acetate	99.28	0.08 ± 0.01	34341.12 ± 3247.92	99.94	0.20 ± 0.13	−1.71 × 10^{-3} ± 1.31 × 10^{-3}	0*	0*
butyl acetate	99.80	0.11 ± 9.14 × 10^{-3}	33568.65 ± 2257.24	99.90	0*	7.82 × 10^{-4} ± 1.03 × 10^{-3}	0*	3.83 × 10^{-9} ± 3.76 × 10^{-9}
methyl propionate	99.53	0.03 ± 2.22 × 10^{-3}	60923.82 ± 2964.81	99.67	0*	0*	0*	0*
ethanol	99.80	0.08 ± 8.53 × 10^{-3}	56639.38 ± 5003.79	99.77	0*	0*	0*	1.80 × 10^{-9} ± 1.59 × 10^{-9}
1-propanol	99.65	0.20 ± 0.04	28025.26 ± 4390.36	99.69	−0.12 ± 0.04	1.25 × 10^{-3} ± 3.95 × 10^{-4}	−4.34 × 10^{-6} ± 1.30 × 10^{-6}	5.03 × 10^{-9} ± 1.43 × 10^{-9}

[a]Standard uncertainty $u(P)$ = 0.3 kPa. [b]0* indicates that the parameter has no significance and is not statistically significant.

The above results were output directly by the statistical analysis software. The above data denoted that the KAT-LSER model fitted the solubility data of EP well, but the Hildebrand solubility parameter (δ_H) was not significant in this model and had no statistical significance, so δ_H was excluded. And from the fitting model, the regression coefficient c_1 of π^* was positive, which implied that the solubility of EP was positively correlated with this parameter. This indicated that the nonspecific polarity/dipolarity of solvents contributed to the dissolution of EP. The negative regression coefficients of α and β indicated that the solubility of EP decreased with the increase of hydrogen bond donor capacity and hydrogen bond acceptor capacity of solvents. That is, the solve−solvent interaction through specific hydrogen bond was not conducive to the dissolution process of EP. From the regression coefficients of π^*, α, and β, the contribution of each parameter to the total solvent effect can be calculated by eq 20, and the following results were obtained: polarity/dipolarity 27.01%, hydrogen bond donor capacity 24.25%, and hydrogen bond acceptor capacity 19.55%. In conclusion, the sum of these coefficients accounted for up to 70.81% of the total solvent effect, demonstrating that the parameters of the KAT-LSER model played a decisive role in the solubility of EP in the selected solvents. Specifically, the solubility of EP in the selected solvents mainly depended on nonspecific polarity/dipolarity.

$$\lambda_i = \frac{c_i}{c_0 + c_1 + c_2 + c_3} \times 100 \tag{20}$$

where λ_i is the contribution rate of each parameter.

4.5. Thermodynamic Properties of the Solution. According to the van't Hoff model, it could be seen that there was a linear relationship between the logarithm of molar solubility of EP ($\ln x_1$) and $(1/T - 1/T_{av})$, so the linear fitting was plotted with $\ln x_1$ as the vertical coordinate and $(1/T - 1/T_{av})$ as the horizontal coordinate, and then the slope $(-\Delta_{sol}H^\circ)/R$ and the intercept b were obtained. The specific results are shown in Figure 6 and Table 7. Table 7 shows that the adjusted R^2 of the models was close to 1, which meant a good fit of the model to the data.

The thermodynamic parameters of EP in 13 pure solvents could be calculated from the fitting results, and the detailed results are displayed in Table 7. From Table 7, it could be observed that $\Delta_{sol}H^\circ$, $\Delta_{sol}S^\circ$, and $\Delta_{sol}G^\circ$ were all positive during the dissolution process of EP, manifesting that the dissolution process of EP in the 13 pure solvents was endothermic, nonspontaneous, and entropy-increasing. In addition, it was also noted that the value of ξ_H/% of 13 pure solvents was greater than the value of ξ_{TS}/%, indicating that $\Delta_{sol}H^\circ$ was the main contributor to $\Delta_{sol}G^\circ$ during the dissolution of EP.

Furthermore, this study has identified certain limitations that warrant further improvement and extension in subsequent research. Regarding thermodynamic modeling, various types of models can be selected to correlate and fit the solubility data of EP. Examples of such models include the Wilson model and the NRTL model. For thermodynamic analysis of solutions, molecular dynamics simulations can be employed to investigate the interactions between eplerenone and solvent molecules, which can dynamically elucidate the relationship between solubility of EP and solvent properties.

https://doi.org/10.1021/acsomega.4c01550
ACS Omega 2024, 9, 21333−21345

Table 6. Deviations of the Modified Apelblat Model, van't Hoff Model, λh Model, and Polynomial Empirical Model (P = 101.3 kPa)[a]

	modified Apelblat model		van't Hoff model		λh model		polynomial empirical model	
solvents	10^2ARD	10^5RMSD	10^2ARD	10^5RMSD	10^2ARD	10^5RMSD	10^2ARD	10^5RMSD
acetonitrile	0.72	16.64	1.23	29.47	0.92	23.92	0.43	9.19
DMF	1.42	7.05	1.47	8.53	1.47	8.50	0.51	3.75
acetone	2.45	4.34	2.73	4.74	2.70	4.67	1.54	3.49
2-butanone	0.62	4.01	0.73	4.18	0.70	4.11	0.53	3.48
4-methyl-2-pentanone	1.82	8.38	1.93	9.72	1.81	9.07	1.17	5.91
ethyl formate	1.54	3.50	3.20	5.78	3.10	5.64	1.35	3.08
methyl acetate	2.04	11.18	1.96	12.91	2.03	13.38	1.76	10.06
ethyl acetate	0.84	3.52	1.30	4.29	1.09	3.82	0.78	3.34
propyl acetate	1.61	3.57	3.77	7.15	3.62	6.86	0.80	1.67
butyl acetate	1.14	1.40	2.20	2.14	2.26	2.21	0.99	1.32
methyl propionate	0.97	4.21	1.66	6.73	1.41	5.85	1.04	4.17
ethanol	2.15	0.57	2.79	0.61	2.81	0.61	2.37	0.56
1-propanol	3.27	0.55	4.70	0.64	4.68	0.64	2.28	0.50

[a]Standard uncertainty $u(P)$ = 0.3 kPa.

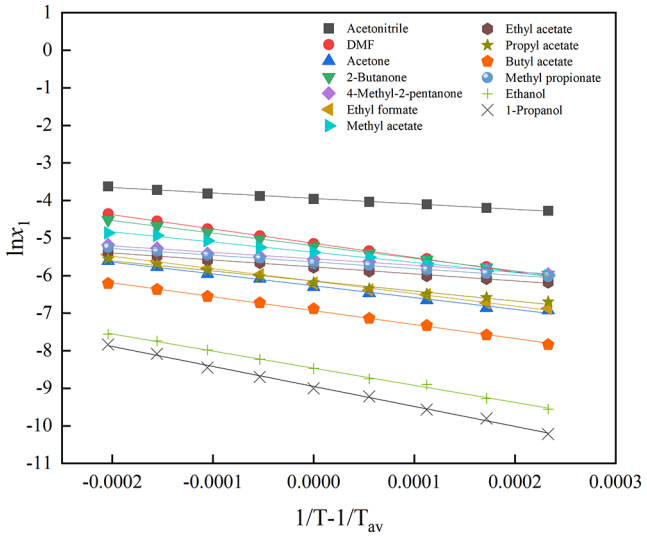

Figure 6. Relationship between the logarithm of the molar solubility ($\ln x_1$) and the reciprocal of temperature ($1/T - 1/T_{av}$) for EP in 13 pure solvents.

5. CONCLUSIONS

The solubility of EP in 13 pure solvents (acetonitrile, DMF, acetone, 2-butanone, 4-methyl-2-pentanone, ethyl formate, methyl acetate, ethyl acetate, propyl acetate, butyl acetate, methyl propionate, ethyl propionate, ethanol, and 1-propanol) was determined by the gravimetric method at atmospheric pressure and temperature of 283.15 to 323.15 K. The following conclusions were drawn from the work. The solubility of EP in the selected solvents was positively correlated with the thermodynamic temperature. In the experimental range, EP had the highest molar solubility in acetonitrile (2.67×10^{-2}, 323.15 K) and the lowest in 1-propanol (3.65×10^{-5}, 283.15 K). The modified Apelblat model, van't Hoff model, λh model, and polynomial empirical model correlated well with the solubility data of EP, but the best model was the λh model, with a minimum ARD of 7.0×10^{-3} and a minimum RMSD of 6.1×10^{-6}. Parameters such as polarity/dipolarity, hydrogen bond donor capacity, and hydrogen bond acceptor capacity accounted for 70.81% of the total solvent effect in KAT-LSER model but mainly depended on nonspecific polarity/dipolarity. The thermodynamic properties ($\Delta_{sol}H°$, $\Delta_{sol}S°$, and $\Delta_{sol}G°$) of the dissolution process of EP in 13 pure solvents were all

Table 7. Thermodynamic Parameters of the Dissolution Process of EP in 13 Pure Solvents (P = 101.3 kPa)[a]

solvents	$100R^2$	intercept	slope	$\Delta_{sol}S°$ (J/(mol·K))	$\Delta_{sol}H°$ (kJ/mol)	$\Delta_{sol}G°$ (kJ/mol)	ξ_H/%	ξ_{TS}/%
acetonitrile	99.52	$-3.95 \pm 5.02 \times 10^{-3}$	-1454.32 ± 35.55	7.06	12.09	9.95	84.96	15.04
DMF	99.87	$-5.14 \pm 6.73 \times 10^{-3}$	-3804.11 ± 47.68	61.58	31.63	12.96	62.88	37.12
acetone	99.21	-6.27 ± 0.01	-3142.01 ± 98.82	34.02	26.12	15.81	71.69	28.31
2-butanone	99.96	$-5.21 \pm 3.25 \times 10^{-3}$	-3354.22 ± 23.02	48.71	27.89	13.12	65.38	34.62
4-methyl-2-pentanone	99.06	$-5.56 \pm 8.38 \times 10^{-3}$	-1719.20 ± 59.33	0.96	14.29	14.00	98.01	1.99
ethyl formate	99.44	-6.15 ± 0.01	-3319.20 ± 87.94	39.89	27.60	15.50	69.53	30.47
methyl acetate	99.61	$-5.38 \pm 8.45 \times 10^{-3}$	-2704.92 ± 59.83	29.46	22.49	13.56	71.58	28.42
ethyl acetate	99.61	$-5.77 \pm 5.82 \times 10^{-3}$	-1857.99 ± 41.20	2.97	15.45	14.55	94.49	5.51
propyl acetate	98.54	-6.15 ± 0.02	-2667.20 ± 114.76	22.05	22.18	15.49	76.84	23.16
butyl acetate	99.73	$-6.94 \pm 9.66 \times 10^{-3}$	-3704.77 ± 68.41	43.94	30.80	17.48	69.81	30.19
methyl propionate	99.36	$-5.64 \pm 7.16 \times 10^{-3}$	-1783.94 ± 50.75	2.05	14.83	14.21	95.98	4.02
ethanol	99.72	-8.47 ± 0.01	-4556.31 ± 85.20	54.56	37.88	21.34	69.61	30.39
1-propanol	99.66	-8.95 ± 0.02	-5320.97 ± 109.63	71.49	44.24	22.57	67.12	32.88

[a]Standard uncertainty $u(P)$ = 0.3 kPa.

https://doi.org/10.1021/acsomega.4c01550
ACS Omega 2024, 9, 21333−21345

positive, indicating that the dissolution process of EP was endothermic, nonspontaneous, and entropy-increasing.

This study provides valuable data on the solubility, dissolution characteristics, and thermodynamic parameters of EP. It offers important insights for the production, crystallization, and purification processes of EP, as well as guidance for optimizing the crystallization of EP in industry.

AUTHOR INFORMATION

Corresponding Author

Jianfang Liu − *School of Life Science and Technology, Wuhan Polytechnic University, Wuhan 430023, China;* orcid.org/0000-0002-7239-8797; Email: jianfang66@126.com

Authors

Ting Liu − *School of Life Science and Technology, Wuhan Polytechnic University, Wuhan 430023, China*

Rongrong Zhang − *School of Life Science and Technology, Wuhan Polytechnic University, Wuhan 430023, China*

Sicheng Yang − *School of Life Science and Technology, Wuhan Polytechnic University, Wuhan 430023, China*

Yaoyun Zhang − *School of Life Science and Technology, Wuhan Polytechnic University, Wuhan 430023, China*

Chenglingzi Yi − *School of Life Science and Technology, Wuhan Polytechnic University, Wuhan 430023, China*

Shuai Peng − *School of Life Science and Technology, Wuhan Polytechnic University, Wuhan 430023, China*

Qing Yang − *School of Life Science and Technology, Wuhan Polytechnic University, Wuhan 430023, China*

Complete contact information is available at: https://pubs.acs.org/10.1021/acsomega.4c01550

Author Contributions

J.L.: Project administration, funding acquisition, writing—review and editing, and supervision. T.L.: Conceptualization, data curation, and writing—original draft. R.Z.: Visualization and investigation. S.Y.: Software and validation. Y.Z.: Methodology. C.Y.: Supervision. S.P.: Data curation. Q.Y.: Resources.

Notes

The authors declare no competing financial interest.

ACKNOWLEDGMENTS

The authors are thankful to Wuhan Research Institute of Materials Protection for providing DSC equipment. The authors are also thankful to Li Yinhua for experimental guidance.

REFERENCES

(1) Azizi, M. Aldosterone receptor antagonists. *Ann. d'Endocrinol.* **2021**, *82* (3−4), 179−181.

(2) Carey, R. M.; Calhoun, D. A.; Bakris, G. L.; Brook, R. D.; Daugherty, S. L.; Dennison-Himmelfarb, C. R.; Egan, B. M.; Flack, J. M.; Gidding, S. S.; Judd, E.; Lackland, D. T.; Laffer, C. L.; Newton-Cheh, C.; Smith, S. M.; Taler, S. J.; Textor, S. C.; Turan, T. N.; White, W. B.; on behalf of the American Heart Association Professional/Public Education and Publications Committee of the Council on Hypertension; Council on Cardiovascular and Stroke Nursing; Council on Clinical Cardiology; Council on Genomic and Precision Medicine; Council on Peripheral Vascular Disease; Council on Quality of Care and Outcomes Research; and Stroke Council. Resistant Hypertension: Detection, Evaluation, and Management: A Scientific Statement From the American Heart Association. *Hypertension* **2018**, *72* (5), e53−e90.

(3) Wang, Z.; Chen, Z.; Zhang, L.; Wang, X.; Hao, G. Status of hypertension in China: results from the China hypertension survey, 2012−2015. *Circulation* **2018**, *137* (22), 2344−2356.

(4) Yang, Q.; Ye, W. D.; Yuan, J. Y.; Nie, J. J.; Xu, D. J. Eplerenone ethanol solvate. *Acta Crystallogr., Sect. E: Struct. Rep. Online* **2008**, *64* (5), o829.

(5) Yang, Q.; Zhang, B. Y.; Ye, W. D.; Yuan, J. Y.; Xu, D. J.; Nie, J. J. Crystal Structure of 9α,11-Epoxy-7α-(methoxycarbonyl)-3-oxo-17α-pregn-4-ene-21,17-carbolactone. *J. Chem. Crystallogr.* **2008**, *38* (9), 659−661.

(6) Dams, I.; Bialonska, A.; Cmoch, P.; Krupa, M.; Pietraszek, A.; Ostaszewska, A.; Chodynski, M. Synthesis and physicochemical characterization of the process-related impurities of eplerenone, an antihypertensive drug. *Molecules* **2017**, *22* (8), 1354 DOI: 10.3390/molecules22081354.

(7) Nabati, M.; Tabiban, S.; Khani, A.; Yazdani, J.; Vafainezhad, H. The effects of spironolactone and eplerenone on left ventricular function using echocardiography in symptomatic patients with new-onset systolic heart failure: a comparative randomised controlled trial. *Heart, Lung Circ.* **2021**, *30* (9), 1292−1301.

(8) Pardo-Martínez, P.; Barge-Caballero, E.; Bouzas-Mosquera, A.; Barge-Caballero, G.; Couto-Mallon, D.; Paniagua-Martin, M. J.; Sagastagoitia-Fornie, M.; Prada-Delgado, O.; Muniz, J.; Almenar-Bonet, L.; Vazquez-Rodriguez, J. M.; Crespo-Leiro, M. G. Real world comparison of spironolactone and eplerenone in patients with heart failure. *Eur. J. Int. Med.* **2022**, *97*, 86−94.

(9) El Mokadem, M.; Abd El Hady, Y.; Aziz, A. A prospective single-blind randomized trial of ramipril, eplerenone and their combination in type 2 diabetic nephropathy. *Cardiorenal Med.* **2020**, *10* (6), 392−401.

(10) Farooq, O.; Habib, A.; Shah, M. A.; Ahmed, N. Effect of oral eplerenone in anatomical and functional improvement in patients with chronic central serous chorioretinopathy. *Pak. J. Med. Sci.* **2019**, *35* (6), 1544−1547, DOI: 10.12669/pjms.35.6.896.

(11) Fasler, K.; Gunzinger, J. M.; Barthelmes, D.; Zweifel, S. A. Routine clinical practice treatment outcomes of eplerenone in acute and chronic central serous chorioretinopathy. *Front. Pharmacol.* **2021**, *12*, No. 675295, DOI: 10.3389/fphar.2021.675295.

(12) Tam, T. S.; Wu, M. H.; Masson, S. C.; Tsang, M. P.; Stabler, S. N.; Kinkade, A.; Tung, A.; Tejani, A. M. Eplerenone for hypertension. *Cochrane Database Syst. Rev.* **2017**, *2017*, No. CD008996.

(13) Bhola, R.; Ghumara, R.; Patel, C.; Parsana, V.; Bhatt, K.; Kundariya, D.; Vaghani, H. Solubility and Thermodynamics Profile of Benzethonium Chloride in Pure and Binary Solvents at Different Temperatures. *ACS Omega* **2023**, *8* (16), 14430−14439.

(14) Baracaldo-Santamaría, D.; Calderon-Ospina, C. A.; Ortiz, C. P.; Cardenas-Torres, R. E.; Martinez, F.; Delgado, D. R. Thermodynamic Analysis of the Solubility of Isoniazid in (PEG 200 + Water) Cosolvent Mixtures from 278.15 K to 318.15 K. *Int. J. Mol. Sci.* **2022**, *23* (17), No. 10190, DOI: 10.3390/ijms231710190.

(15) Yang, C.; Yan, H.; Huang, Q.; Yang, W.; Hu, Y. Solubility Determination and Thermodynamic Model Analysis of Esculetin in Different Solvents from 273.15 to 318.15 K. *J. Chem. Eng. Data* **2024**, *69* (4), 1546−1556, DOI: 10.1021/acs.jced.3c00771.

(16) Kooshkebaghi, F.; Jabbari, M.; Farajtabar, A. A study on the solubility of some amino acids in (H_2O + EtOH) and (H_2O + EtOH + NaI) systems by gravimetric method at T = 298.15 K: Experimental measurements and COSMO-RS calculations. *J. Mol. Liq.* **2024**, *398*, No. 124229.

(17) Yaws, C. L. Solubility parameter, liquid volume, and van der waals area and volume. In *Chemical Properties Handbook*; McGraw-Hill Professional: New York, 1999.

(18) https://www.chemspider.com/Chemical-Structure.10203511.html.

(19) Nishiyama, K.; Sakiyama, M.; Seki, K. Enthalpies of Combustion of Organic Compouds. V. 3- and 4-Nitroanilines. *Bull. Chem. Soc. Jpn.* **1983**, *56* (10), 3171−3172.

(20) Yu, C.; Sun, X.; Wang, Y.; Du, S.; Shu, L.; Sun, Q.; Xue, F. Determination and Correlation of Solubility of Metformin Hydro-

chloride in Aqueous Binary Solvents from 283.15 to 323.15 K. *ACS Omega* **2022**, *7* (10), 8591−8600.
(21) Pinho, S. P.; Macedo, E. A. Solubility of NaCl, NaBr, and KCl in Water, Methanol, Ethanol, and Their Mixed Solvents. *J. Chem. Eng. Data* **2005**, *50* (1), 29−32.
(22) Apelblat, A.; Manzurola, E. Solubilities of o-acetylsalicylic, 4-aminosalicylic, 3,5-dinitrosalicylic, and p-toluicacid, and magnesium-DL-aspartate in water from T = (278 to 348) K. *J. Chem. Thermodyn.* **1999**, *31*, 85−91.
(23) Wang, Z.; Yu, S.; Li, H.; Liu, B.; Xia, Y.; Guo, J.; Xue, F. Solid−Liquid Equilibrium Behavior and Solvent Effect of Gliclazide in Mono- and Binary Solvents. *ACS Omega* **2022**, *7* (42), 37663−37673.
(24) Li, M.; Gao, Z.; Li, Z.; Wang, Z.; Zhou, R.; Wang, B. Determination and correlation of solubility of 4,4′-difluorobenzophenone in pure and binary mixed solvents and thermodynamic properties of solution. *J. Mol. Liq.* **2020**, *317*, No. 113903, DOI: 10.1016/j.molliq.2020.113903.
(25) Buchowski, H.; Ksiazczak, A.; Pietrzyk, S. Solvent activity along a saturation line and solubility of hydrogen-bonding solids. *J. Phys. Chem. A* **1980**, *84*, 975−979.
(26) Guo, H.-j.; Cao, D.-l.; Liu, Y.; Dang, X.; Yang, F.; Li, Y.-x.; Hu, W.-h.; Jiang, Z.-m.; Li, Z.-h. Determination and correlation of solubility of N-methyl-3,4,5-trinitropyrazole (MTNP) in ten pure solvents from 283.15 K to 323.15 K. *Fluid Phase Equilib.* **2017**, *444*, 13−20.
(27) Yang, F.; Li, Y.-x.; Dang, X.; Chai, X.-x.; Guo, H.-j. Determination and correlation of solubility of 2,2′,4,4′,6,6′-hexanitro-1,1′-biphenyl and 2,2′,2″,4,4′,4″,6,6′,6″-Nonanitro-1,1′:3′,1″-terphenyl in six pure solvents. *Fluid Phase Equilib.* **2018**, *467*, 8−16.
(28) Li, C.; Li, Y.; Gao, X.; Lv, H. Rutaecarpine dissolved in binary aqueous solutions of methanol, ethanol, isopropanol and acetone: Solubility determination, solute-solvent and solvent-solvent interactions and preferential solvation study. *J. Chem. Thermodyn.* **2020**, *151*, No. 106253, DOI: 10.1016/j.jct.2020.106253.
(29) Endo, S.; Goss, K.-U. Applications of Polyparameter Linear Free Energy Relationships in Environmental Chemistry. *Environ. Sci. Technol.* **2014**, *48* (21), 12477−12491.
(30) Huang, W.; Wang, H.; Li, C.; Wen, T.; Xu, J.; Ouyang, J.; Zhang, C. Measurement and correlation of solubility, Hansen solubility parameters and thermodynamic behavior of Clozapine in eleven mono-solvents. *J. Mol. Liq.* **2021**, *333*, No. 115894, DOI: 10.1016/j.molliq.2021.115894.
(31) Kamlet, M. J.; Abboud, J.-L. M.; Abraham, M. H.; Taft, R. W. Linear solvation energy relationships. 23. a comprehensive collection of the solvatochromic parameters, π^*, α, and β, and some methods for simplifying the generalized solvatochromic equation. *J. Org. Chem.* **1983**, *48*, 2877−2887.
(32) Park, J. H.; Lee, Y. K.; Cha, J. S.; Kim, S. K.; Lee, Y. R.; Lee, C.-S.; Carr, P. W. Correlation of gas−liquid partition coefficients using a generalized linear solvation energy relationship. *Microchem. J.* **2005**, *80* (2), 183−188.
(33) Maitra, A.; Bagchi, S. Study of solute−solvent and solvent−solvent interactions in pure and mixed binary solvents. *J. Mol. Liq.* **2008**, *137* (1−3), 131−137.
(34) Rezaei, H.; Rahimpour, E.; Zhao, H.; Martinez, F.; Jouyban, A. Solubility measurement and thermodynamic modeling of caffeine in N-methyl-2-pyrrolidone + isopropanol mixtures at different temperatures. *J. Mol. Liq.* **2021**, *336*, No. 116519, DOI: 10.1016/j.molliq.2021.116519.
(35) Xu, H.; Kang, L.; Qin, J.; Lin, J.; Xue, M.; Meng, Z. Solubility of Azilsartan in Methanol, Ethanol, Acetonitrile, n-Propanol, Isopropanol, Tetrahydrofuran, and Binary Solvent Mixtures between 293.15 and 333.15 K. *ACS Omega* **2020**, *5* (11), 6141−6145.
(36) Alshehri, S.; Hussain, A.; Ahsan, M. N.; Ali, R.; Siddique, M. U. M. Thermodynamic, Computational Solubility Parameters in Organic Solvents and In Silico GastroPlus Based Prediction of Ketoconazole. *ACS Omega* **2021**, *6* (7), 5033−5045.
(37) Kalam, M. A.; Alshamsan, A.; Alkholief, M.; Alsarra, I. A.; Ali, R.; Haq, N.; Anwer, M. K.; Shakeel, F. Solubility Measurement and Various Solubility Parameters of Glipizide in Different Neat Solvents. *ACS Omega* **2020**, *5* (3), 1708−1716.
(38) Roy, S.; Rigaa, A. T.; Alexander, K. S. Experimental design aids the development of a differential scanning calorimetry standard test procedure for pharmaceuticals. *Thermochim. Acta* **2002**, *392-393*, 399−404.
(39) Yassin, G. E.; Khalifa, M. K. A. Development of eplerenone nano sono-crystals using factorial design: enhanced solubility and dissolution rate via anti solvent crystallization technique. *Drug Dev. Ind. Pharm.* **2022**, *48* (12), 683−693.
(40) Gu, C.-H.; Li, H.; Gandhi, R. B.; Raghavan, K. Grouping solvents by statistical analysis of solvent property parameters: implication to polymorph screening. *Int. J. Pharm.* **2004**, *283* (1−2), 117−125.

https://doi.org/10.1021/acsomega.4c01550
ACS Omega 2024, 9, 21333−21345